Washington University School of Medicine
Digital Commons@Becker

Open Access Publications

2015

# Ribosomes slide on lysine-encoding homopolymeric A stretches.

Kristin S. Koutmou
*Johns Hopkins University*

Anthony P. Schuller
*Johns Hopkins University*

Julie L. Brunelle
*Howard Hughes Medical Institute*

Aditya Radhakrishnan
*Johns Hopkins University*

Sergej Djuranovic
*Washington University School of Medicine in St. Louis*

***See next page for additional authors***

Follow this and additional works at: http://digitalcommons.wustl.edu/open_access_pubs

Recommended Citation
Koutmou, Kristin S.; Schuller, Anthony P.; Brunelle, Julie L.; Radhakrishnan, Aditya; Djuranovic, Sergej; and Green, Rachel, ,"Ribosomes slide on lysine-encoding homopolymeric A stretches.." Elife.,. 1-51. (2015).
http://digitalcommons.wustl.edu/open_access_pubs/3720

This Open Access Publication is brought to you for free and open access by Digital Commons@Becker. It has been accepted for inclusion in Open Access Publications by an authorized administrator of Digital Commons@Becker. For more information, please contact engeszer@wustl.edu.

**Authors**
Kristin S. Koutmou, Anthony P. Schuller, Julie L. Brunelle, Aditya Radhakrishnan, Sergej Djuranovic, and Rachel Green

This open access publication is available at Digital Commons@Becker: http://digitalcommons.wustl.edu/open_access_pubs/3720

ACCEPTED MANUSCRIPT

# Ribosomes slide on lysine-encoding homopolymeric A stretches

Kristin S Koutmou, Anthony P Schuller, Julie L Brunelle, Aditya Radhakrishnan, Sergej Djuranovic, Rachel Green

DOI: http://dx.doi.org/10.7554/eLife.05534

Cite as: eLife 2015;10.7554/eLife.05534

Received: 9 November 2014
Accepted: 18 February 2015
Published: 19 February 2015

This PDF is the version of the article that was accepted for publication after peer review. Fully formatted HTML, PDF, and XML versions will be made available after technical processing, editing, and proofing.

Stay current on the latest in life science and biomedical research from eLife.
Sign up for alerts at elife.elifesciences.org

**Ribosomes slide on lysine-encoding homopolymeric A stretches**

Kristin S. Koutmou[1], Anthony P. Schuller[1], Julie L. Brunelle[1,2], Aditya Radhakrishnan[1], Sergej Djuranovic[3], Rachel Green[1,2,4]

[1]Johns Hopkins School of Medicine, Department of Molecular Biology and Genetics. 725 N. Wolfe Street, Baltimore, MD 21205.

[2] Howard Hughes Medical Institute

[3] Washington University School of Medicine, Department of Cell Biology and Physiology. 60 South Euclid Avenue, Campus Box 8228, St. Louis, MO 63110.

[4] Corresponding author

**Abstract**

Protein output from synonymous codons is thought to be equivalent if appropriate tRNAs are sufficiently abundant. Here we show that mRNAs encoding iterated lysine codons, AAA or AAG, differentially impact protein synthesis: insertion of iterated AAA codons into an ORF diminishes protein expression more than insertion of synonymous AAG codons. Kinetic studies in *E. coli* reveal that differential protein production results from pausing on consecutive AAA-lysines followed by ribosome sliding on homopolymeric A sequence. Translation in a cell free-expression system demonstrates that diminished output from AAA-codon-containing reporters results from premature translation termination on out of frame stop codons following ribosome sliding. In eukaryotes, these premature termination events target the mRNAs for Nonsense-Mediated-Decay (NMD). The finding that ribosomes slide on homopolymeric A sequences explains bioinformatic analyses indicating that consecutive AAA codons are under-represented in gene-coding sequences. Ribosome 'sliding' represents an unexpected type of ribosome movement possible during translation.

## Introduction

Messenger RNA (mRNA) transcripts can contain errors that result in the production of incorrect protein products**.** Both bacterial and eukaryotic cells have evolved mechanisms to deal with such errors which involve (1) proteolytic degradation of the aberrant protein product, (2) mRNA decay and (3) ribosome rescue (Shoemaker and Green 2012). One such mRNA surveillance pathway in eukaryotes targets mRNAs that lack stop codons (Non-Stop-Decay or NSD). In these cases, actively translating ribosomes are thought to read into the 3' terminal poly(A) sequence of the mRNA triggering ribosome pausing as poly-lysine is translated, followed by the recruitment of ubiquitin ligases, mRNA decay and ribosome recycling factors (review (Klauer and van Hoof 2012)). Given the substantial amount of premature (or alternative) polyadenylation that has been documented in eukaryotes (Ozsolak et al. 2010), it seems that such an mRNA surveillance pathway might have considerable biological significance. Similarly, in bacteria, while no "NSD-like" response has been characterized, it is known that poly(A) sequences are added to mRNAs in the process of being degraded (review (Dreyfus and Regnier 2002)), and so ribosomes on these mRNAs may encounter similar challenges. The utilization in bacteria and eukaryotes of 3' poly(A) tails as non-coding elements may reflect a common solution to the challenges for the ribosome in translating such sequences.

Most studies investigating how NSD works have been conducted in yeast using reporter constructs. Early studies in *S. cerevisiae* revealed that mRNAs lacking stop-codons are targeted for decay both in a reaction dependent on the exosome-associated factor Ski7 (van Hoof et al. 2002) and in a more canonical degradation reaction involving decapping and 5' to 3'

exonucleolytic degradation (Frischmeyer et al. 2002). Other factors involved in NSD have since been discovered including Dom34 and Hbs1 which facilitate ribosome rescue during NSD (Izawa et al. 2012; Tsuboi et al. 2012), Ltn1 and Not4 which ubiquitinate the protein products on non-stop mRNAs (Dimitrova et al. 2009; Bengtson and Joazeiro 2010), and a number of other factors genetically identified as critical for poly-basic-mediated stalling (Brandman et al. 2012; Chiabudini et al. 2014; Kuroha et al. 2010). Although many players in NSD have been identified and their functions defined, there remain critical gaps in our understanding.

In this manuscript, we focus on what must be the earliest events in NSD, the translation of poly-lysine sequences by the ribosome. NSD is widely thought to be triggered by unfavorable electrostatic interactions that occur in the ribosomal exit tunnel when ribosomes translate the poly(lysine) sequences encoded by poly(A). Indeed, biochemical studies in rabbit reticulocyte lysate with proteins interrupted by iterated poly-lysine and poly-arginine sequences indicate that positively charged residues do slow translation and produce transiently arrested species (Lu and Deutsch 2008). Other examples of peptide-mediated stalling have also been documented in bacterial and eukaryotic systems. In some cases, such as the *tnaC* gene, *secM*, or *ermCL* in bacteria, the peptide stalling motif is several amino acids in length and appears to specifically engage the contours of the exit tunnel to elicit stalling (Gong and Yanofsky 2002; Nakatogawa and Ito 2002; Vazquez-Laslop et al. 2008; Seidelt et al. 2009; Bhushan et al. 2011; Ito and Chiba 2013; Arenz et al. 2014). Polyproline sequences have recently been shown to cause stalling during translation in bacteria and eukaryotes in the absence of specialized bypass factors, EFP and eIF5A, respectively (Doerfel et al. 2013; Gutierrez et al. 2013; Ude et al. 2013).

In this case, proline is thought to adopt a conformation that interferes with the ribosome active site geometry.

Here we take a high-resolution biochemical look at the molecular events that occur when the ribosome translates poly(lysine) peptides. We find that insertion of consecutive AAA lysine codons into reporters has a stronger negative impact on protein expression than insertion of an equivalent number of AAG lysine codons in both eukaryotes and bacteria. Kinetic and toe-printing studies in an *in vitro* reconstituted *E. coli* translation system reveal that differential protein output is the downstream consequence of ribosome pausing followed by an unanticipated ribosome movement on successive AAA codons that we refer to as "sliding". When sliding occurs in the middle of genuine ORFs in a cell, frame is lost and ribosomes encounter out of frame stop codons that result in canonical (stop-codon mediated) termination. In eukaryotes, such premature termination events target the mRNA for NMD. The finding that the ribosome can robustly slide on poly(A) sequences explains bioinformatic analyses revealing that consecutive AAA codons are under-represented in ORFs in all genomes (Arthur et al. 2014) and helps to rationalize the widespread usage of poly(A) sequence as a regulatory rather than a coding feature.

## Results

### Protein production is differentially diminished by iterated lysine codons (AAA vs. AAG)

To begin investigating the translation of poly(lysine)-encoding sequences, we created a series of mCherry- and luciferase-based reporter constructs (Figure 1A) containing no insert, glutamic acid (GAA) repeats, or consecutive lysine residues encoded by various combinations of

AAA and AAG codons. These reporters were introduced into *S. cerevisiae* and *E. coli* cells and the protein products visualized by either luminescence or fluorescence, respectively (Figure 1B). The insertion of twelve consecutive negatively charged glutamic acid residues (GAA) had no negative impact on production of the reporter protein (Figure 1B). By contrast, the addition of consecutive lysine residues generally resulted in overall less protein production (Figure 1B), consistent with previous studies of poly(lysine) containing reporters (Ito-Harashima et al. 2007; Chiabudini et al. 2012; Lu and Deutsch 2008). Interestingly, we find that protein output from the poly(lysine)-containing reporters is codon dependent in both bacteria and yeast; reporters containing iterated AAG lysine codons generate more protein than those with an equivalent number of synonymous AAA codons (Figure 1B). The relative differences in expression of AAG- vs. AAA-encoded poly(lysine)-containing reporters in *E. coli* and *S. cerevisiae* are comparable (4 $\pm$ 0.3-fold more in *E. coli* and 3 $\pm$ 1-fold more in *S. cerevisiae* from reporters with $AAG_{12}$ versus $AAA_{12}$).

**Kinetic analysis of lysine incorporation on consecutive AAA and AAG codons**

One potential explanation for the codon-dependent expression of poly(lysine)-containing proteins could be that the ribosome more rapidly incorporates lysine on AAG than AAA codons. In *E. coli* a single tRNA with a UUU anti-codon decodes both lysine codons (Chan and Lowe 2009), making *E. coli* an excellent system for studying differences in the production of poly(lysine) peptides. We measured the rate of lysine incorporation using a previously described reconstituted *E. coli* translation system (Zaher and Green 2009; Youngman et al. 2004; Gromadski et al. 2006) on a series of lysine-encoding simple mRNAs including: AUG-AAA-

112 UUC-AAG-UAA (MKFK-Stop), AUG-UUC-AAA (MFK), AUG-(AAA or AAG)$_5$-UAA (MK$_{(A\ or\ G)5}$-Stop).
113 Only Lys-tRNA$^{Lys}$ was included during the translation of MKFK-Stop and MK$_5$-Stop mRNAs while
114 both Lys-tRNA$^{Lys}$ and Phe-tRNA$^{Phe}$ were present when MFK was translated. Electrophoretic TLC
115 readily resolved the reaction products allowing for analysis of intermediate and complete
116 peptide products (Figure 2A). The quantitated data were modeled in Mathematica using the
117 kinetic scheme displayed in Figure 2B (see Material and Methods). These experiments reveal
118 that addition of a single lysine in a heteropolymeric sequence is rapid and independent of
119 whether lysine is the first or second amino acid incorporated (Figure 2C, rate constants for
120 formation of MK and MFK peptides are 12 $s^{-1}$ and 7 $s^{-1}$, respectively); these rates are similar to
121 those typically measured for peptide bond formation in this *in vitro* system (Gromadski et al.
122 2006). For messages containing iterated lysine codons, the rate constant for translating the first
123 lysine codon is similarly fast ($k_{1,obs}$ from 2-19 $s^{-1}$, Figure 2C) for AAA and AAG codons. However,
124 subsequent lysines in an iterated sequence are added with considerably slower kinetics on both
125 AAA ($k_{2,obs}$ = 0.0005 and $k_{3,obs}$ = 0.0003 $s^{-1}$) and AAG codons ($k_{2,obs}$ = 0.009 and $k_{3,obs}$ = 0.015 $s^{-1}$)
126 (Figure 2C). We note that the rate of second lysine addition during the translation of MK$_5$-STOP
127 messages are somewhat slower on AAA relative to AAG codons, potentially partially explaining
128 the decreased overall protein output on these mRNAs. More importantly, however, these data
129 show that the reactivity of the second Lys-tRNA$^{Lys}$ on iterated lysine containing messages (such
130 as MK$_5$-Stop) is substantially reduced (at least 130-fold) on both lysine codon-containing mRNAs
131 relative to normal elongation rates. Interestingly, the addition of a second lysine to messages
132 with fewer sequential lysine codons (such as MK$_2$F-STOP) does not exhibit such a striking kinetic
133 defect ($k_{2,obs}$ is not largely affected, data not shown). These data suggest that the identity of the

message (i.e. a long polyA sequence) plays a critical role in the observed slowing of elongation. Toe-printing assays performed using the *E. coli* PURE cell-free translation system are consistent with these observations; *E. coli* ribosomes stall when the second lysine codon in iterated (AAA)- and (AAG)-codon containing sequences is positioned in the A site (Figure 2 – figure supplement 1). Together, these results reveal that translating consecutive lysines in a poly-lysine peptide sequence, either on iterated AAA or AAG codons, can lead to substantial kinetic delays *in vitro*.

### *E. coli* ribosomes add extra lysines on iterated AAA-containing mRNAs

As we explored the kinetics of lysine incorporation, we evaluated the ability of the ribosome to translate a variety of $MK_{(A\ or\ G)2}$ di-lysine messages (Figure 3A). Unexpectedly, we found that messages containing iterated AAA codons generate extended peptides longer than the designed coding sequence (Figure 3A). When *E. coli* initiation complexes (programmed with fMet-$tRNA^{fMet}$) are reacted with Lys-$tRNA^{Lys}$ on messages containing two consecutive lysine codons followed by a variety of non-lysine codons (Phe (UUC), Val (GUC), or Stop (UAA)), only MKK peptide should be synthesized. However, we see the formation of a majority population of extended peptide product containing at least four lysines on all messages with two consecutive AAA codons (Figure 3B, lanes 2-4). In contrast, equivalent messages with two AAG codons predominantly form the expected MKK product (Figure 3B, compare lane 3 vs 5). We also find that a mixed sequence of lysine codons (AAA-AAG) can form some extended peptide (Figure 3 – figure supplement 1). These data suggest that 5 As in a row are sufficient to promote the addition of extra lysines *in vitro*. We note that the identity of the codon that follows the di-

lysine sequence is not relevant to the observed amount of extended peptide product (Figure 3B, Figure 3 – figure supplement 2).

The production of peptide products containing more than the encoded number of lysines is surprising, especially given that there are no nearby upstream or downstream in-frame or out-of-frame lysine codons in these mRNAs (Figure 3A). We speculate that these extended peptides result from the ribosome repeatedly moving backwards by at least three nucleotides to position an AAA Lys codon in the A site, and then subsequent standard peptide bond formation. Toe-printing assays performed on iterated AAA- and AAG-containing mRNAs provide further support for such irregular movement of ribosomes specifically on iterated AAA codons (Figure 2 – figure supplement 1); the toeprint on the iterated AAA sequence is diffuse relative to the discrete toeprint seen on iterated AAG sequence. In the course of performing our experiments we carefully considered reports suggesting that T7 RNA polymerase could promiscuously add extra adenosines to poly(A) messages (Tsuchihashi and Brown 1992; Ratinier et al. 2008); no experiment that we performed revealed any evidence for such heterogeneity in our mRNA products (Figure 3- figure supplement 3). Unlike better studied -1 and +1 frameshifting events, these data suggest that ribosomes on iterated AAA sequences are making unexpected and large excursions from their initial frame; we refer to this process as 'ribosome sliding'.

**Ribosome sliding is slow relative to the rate of normal elongation and termination reactions**

The observation of ribosome sliding on iterated AAA codons is surprising given that the ribosome must somewhat regularly translate mRNA sequences *in vivo* that contain two

consecutive AAA codons. While three or more AAA codons in a row are selected against in gene coding sequences, there are thousands of examples of two consecutive AAA codons in *S. cerevisiae* and *E. coli* genes (see further details in bioinformatic analysis below, Table 1). In the experiments described in Figure 3A, ribosome initiation complexes on the specified $MK_{A2}$-Stop and $MK_{A2}F$-Stop messages (Figure 3B) were only supplied with Lys-$tRNA^{Lys}$ and essential elongation factors; the subsequent substrates normally present *in vivo* after the formation of MKK peptide were left out. To determine if ribosome sliding occurs in more typical circumstances, we performed elongation reactions on the same mRNAs, but where both Lys-$tRNA^{Lys}$ and the relevant other downstream substrates (release factor 1 (RF1) or Phe-$tRNA^{Phe}$) were added to the ribosome initiation complexes. The result is clear; in this latter case, the anticipated MKKF or MKK peptide products are predominantly generated (Figure 3C, Figure 3-figure supplement 2). These data suggest that ribosome sliding on iterated AAA sequences occurs more slowly than the normal rate of peptidyl transfer with Phe-$tRNA^{Phe}$ or RF1-catalyzed peptide release, respectively. Moreover, these results readily explain how the ribosome can normally translate (at least two) sequential AAA codons *in vivo* without sliding. When there are more than two AAA codons in a row, each lysine after the first is added slowly (Figure 2B), raising the possibility that sliding may become relevant on such messages.

**Ribosomes slide on poly(A)-containing reporters in an *E. coli* cell free translation system**

The initial *in vivo* observation that protein production is more severely impacted by iterated AAA than AAG codons (Figure 1) was recapitulated using the PURExpress *E. coli* cell free translation system (NEB) (Figure 4A). This system contains all factors required for normal

translation, but lacks cellular factors involved in the degradation of RNA or proteins that might obscure interesting effects on translation. When the mCherry reporters (described in Figure 1A) were expressed in this system, we find that iterated AAA-containing reporters produce less protein than their iterated AAG-containing counterparts (Figure 4A, lanes 3 vs 4). Additionally, we note the appearance of a truncated protein product generated from the iterated AAA-containing reporter (Figure 4A, lane 3). This band is slightly larger than the size of protein produced when a stop-codon is positioned at the insertion site (Figure 4A, lanes 2-3).

To ask whether the truncated band is the typical product of a stalled ribosome, a peptidyl-tRNA, we subjected the products of our PURE reactions to RNase A treatment (Figure 4B). As a positive control, we observed that peptidyl-tRNA product generated from a non-stop mRNA (Figure 4B, lanes 9-10) does indeed change in mobility when treated with RNase A (see uppermost band resolve into smaller peptide products from this inefficiently translated mRNA). By contrast, the truncated band generated from the $(AAA)_{12}$-containing reporter does not shift in mobility on a gel following RNase A treatment (Figure 4A, lanes 5-6). We closely examined our reporter sequence and found that there are several out of frame stop-codons following the $(AAA)_{12}$ insert (Supplementary file 1). We next showed that the truncated band is generated by RF-mediated peptide release, likely on a canonical stop codon reached following ribosome sliding on poly(A) sequence (Figure 4A, lanes 7-8). Further experiments indicate that both RF1 and RF2 can promote release of this product and that the release reaction is independent of RF3 (Figure 4 - figure supplement 1). The formation of truncated product from our $(AAA)_{12}$ reporters is a signature that reports on ribosome sliding on iterated AAA sequences. We note that the truncated band is also observed when the mCherry reporter is expressed in *E. coli* (and

a western is performed with an α-HA antibody) (Figure 4 – figure supplement 2). Together, these data provide evidence that ribosome slipping on iterated AAA sequences occurs both in a fully reconstituted translation system and in *E. coli*.

**Efficiency of ribosome sliding is dictated by consecutive A residues in the mRNA**

To determine the minimum number of consecutive lysine or adenosine residues necessary for ribosomes to robustly slide on the iterated AAA-containing reporters, we expressed reporter constructs containing 3, 6, 9 or 12 lysines (encoded by AAA) in the PURExpress *E. coli* cell free translation system (Figure 5). Truncated product (which we have determined to be a signature of ribosome sliding) was generated with as few as three consecutive lysines. We next asked whether the number of lysines residues or the number of consecutive adenosine nucleotides determines the extent of ribosome sliding. In this case, reporters were created containing a three lysine ($K_3$) insert encoded by 9, 10, 11, or 13 As in a row (Figure 5). We find that an $A_{11}$ repeat results in the robust formation of truncated product (Figure 5, Figure 5 – figure supplement 1) while little product is seen with $A_9$ or $A_{10}$ sequences, though each sequence encodes the same number of consecutive lysines.

**Poly-lysine inserts that promote ribosome sliding are targeted by NMD in *S. cerevisiae***

In eukaryotic systems, NMD is a quality control system that recognizes mRNAs containing premature termination codons (PTC) and targets them for degradation. Upf1 is a key protein in NMD and *upf1*Δ cells stabilize PTC-containing transcripts. Previous studies established that when ribosomes frameshift during translation, these mRNAs are typically targeted for decay by NMD because the ribosomes generally encounter an out of frame

239 premature termination codon (Belew et al. 2011; Belew et al. 2014). We proposed that if the
240 ribosome slides on iterated AAA-containing mRNAs in yeast, as it does in the bacterial system,
241 then iterated AAA-containing mRNAs should be targeted by NMD. We addressed this possibility
242 by measuring the levels of $(AAA)_{12}$, $(AAG)_{12}$, and $(AAGAAGAAA)_4$-containing mRNAs in two
243 different yeast-expressed reporter systems (Figure 1A) in wild-type and *upf1*Δ cells.

244 First, as a control, we measured the mRNA levels of luciferase reporters containing no
245 insert, an engineered premature stop codon (positive control), and a stem-loop known to
246 trigger an alternative mRNA quality control pathway, no-go decay (negative control) (Doma and
247 Parker 2006). We find that the levels of mRNA for PTC and stem-loop containing reporters are
248 lowered (PTC = 2 fold, stem-loop = 21 fold) relative to reporters with no insert in wild-type
249 yeast cells. Moreover, as expected, the level of PTC, but not stem-loop-containing, mRNA is
250 recovered when the reporters are expressed in *upf1*Δ cells (Figure 6A). When this same
251 experiment was performed with a luciferase reporter containing an $(AAA)_{12}$ sequence, we find
252 that reporter mRNA levels are substantially reduced in wild-type cells (> 50-fold down), and
253 that these levels are partially recovered in a *upf1*Δ strain (Figure 6A). These results suggest that
254 the $(AAA)_{12}$-containing reporter is indeed a target of NMD *in vivo*.

255 To more directly compare our *S. cerevisiae* and *E. coli* results, we performed
256 experiments instead using the related mCherry reporters (Figure 1A) with no insert, or a variety
257 of lysine inserts ($(AAG)_{12}$, $(AAA)_{12}$, and $(AAGAAGAAA)_4$). In addition to measuring the absolute
258 levels of reporter mRNAs in wild-type and *upf1*Δ cells (Figure 6), we asked whether the rates of
259 mRNA decay for these reporters are impacted in the *upf1*Δ knock-out background (Figure 6B

and Figure 6 – figure supplement 1). We chose to include a mixed AAA/AAG reporter in addition to the simpler AAA and AAG repeat reporters because this sequence is commonly used to report on the NSD phenomenon (Dimitrova et al. 2009; Chiabudini et al. 2012; Chiabudini et al. 2014). Indeed, a recent study with an $(AAGAAGAAA)_4$-containing reporter argued that a truncated product generated by such a construct resulted from an unusual release factor-dependent termination event on a sense (lysine) codon (Chiabudini et al. 2014). In an attempt to recapitulate these results, we directly looked for evidence of eRF1:eRF3-mediated termination activity on iterated lysine mRNAs *in vitro* using a yeast reconstituted translation system (Shoemaker et al. 2010); we see no evidence that such an event can occur (Figure 6 – figure supplement 2). We propose that an alternative explanation for the published data could be that the ribosome slides out of frame on the $(AAGAAGAAA)_4$ sequence, resulting in premature termination on a previously out-of-frame stop codon, akin to what we observe in the PURE *E. coli* cell free translation system (Figure 4C). This possibility seemed particularly likely given that we observed sliding activity on a AUG-AAA-AAG-UUC-STOP sequence in our *in vitro* reconstituted *E. coli* system (Figure 3- figure supplement 1).

In wild type and *upf1*Δ cells, we find that the level of the $(AAG)_{12}$ containing reporter mRNA is unchanged relative to the mCherry reporter with no insert (Figure 6B). In contrast, the levels of $(AAGAAGAAA)_4$ and $(AAA)_{12}$ reporter mRNAs are significantly reduced compared to the control (no insert) reporter (15-fold and 30-fold, respectively). These observations are consistent with the low levels of protein expressed *in vivo* from these reporters relative to sequences containing no insert or $(AAG)_{12}$ (Figure 1B). As with the luciferase reporters, the level of mCherry mRNA containing an $(AAA)_{12}$ insert is partially recovered by the deletion of *UPF1*

(Figure 6B). Strikingly, when the $(AAGAAGAAA)_4$-containing reporters are expressed in *upf1*Δ cells, the mRNA levels are nearly fully recovered. The mRNA half-lives for these reporters are similarly recovered in the *upf1*Δ cells (Figure 6 - figure supplement 1). Thus both the $(AAGAAGAAA)_4$ and $(AAA)_{12}$ reporter mRNAs are targeted by NMD in yeast cells (Figure 6B). These results are consistent with a model invoking ribosome sliding followed by recognition of out-of-frame premature termination codons.

**Iterated AAA codons are selected against in yeast and bacteria coding regions**

We performed bioinformatic analyses of fully annotated ORFs to evaluate the codon usage in sequences of consecutive lysines found in the *E. coli* and *S. cerevisiae* transcriptomes. In both organisms, AAA codons are found more commonly than AAG codons (62% AAA vs 38% AAG in yeast, and 72% AAA vs 28% AAG in bacteria); however, consecutive AAA codons are under-represented relative to their overall codon usage (Table 1). This is highlighted by the observation that the longer the stretch of lysines, the lower the likelihood of the motif being comprised solely of AAA codons (Table 1). Such an underrepresentation of AAA codons becomes pronounced in runs of 3 or 4 lysine codons in both organisms. In *E. coli*, only a single AAA-AAA-AAA sequence is present, which is 50-fold less common than expected based on the frequency of AAA codons; in contrast, $(AAG)_3$ sequences are found 3.3-fold more often than expected. In *S. cerevisiae,* the trends are similar; there are 2.3 and 4-fold fewer $(AAA)_3$ and $(AAA)_4$ sequences, respectively, than expected. Conversely, $(AAG)_3$ and $(AAG)_4$ sequences are 3 to 5-fold more abundant than expected. These data together argue that evolution has selected against the use of long runs of A to encode sequential lysines within ORFs.

## Discussion

Although many of the major players in NSD have been identified, a high-resolution mechanistic understanding of how translation of poly(A) sequences triggers NSD has been missing. Here, we provide mechanistic insight into what initially happens when the ribosome encounters poly(A) sequence. First, we find that the expression of proteins containing poly-lysine stretches is codon-dependent in both bacteria and eukaryotes, with reporters containing iterated AAA codons consistently producing less protein than those with equivalent AAG codons (Figures 1, 4). This differential protein output is not the result of imprecise RNA polymerase action (Figure 3- figure supplement 3) nor likely of disparities in the rate of adding lysine codons (Figure 2); lysines are slowly incorporated on iterated AAA and AAG codons. Instead, the codon-dependent disparity primarily stems from an unusual sliding event that occurs when ribosomes encounter consecutive AAA codons (Figures 3, 4). Our observation that ribosomes can slide in multiple frames on iterated AAA sequences provides a rationale for consecutive AAA codons being substantially under-represented in open reading frames in most genomes (see Bioinformatic discussion below, Table 1 and (Arthur et al. 2014)).

Our biochemical data in *E. coli* lead us to propose a model (Figure 7) for what happens to the ribosome during the translation of homopolymeric A sequences. On these messages, the first lysine is added quickly ($k_{1,obs}$) while subsequent lysines are added more slowly, causing the ribosome to pause. We note that the rate constants measured in the *in vitro* assay reflect all of the processes that can occur each time a new lysine moiety is added to the growing polypeptide chain (Lys-tRNA$^{Lys}$ binding, peptidyl-transfer, translocation, peptidyl-tRNA drop-off,

70S complex instability, etc). We suspect it to be unlikely that ribosome pausing is caused solely by dramatically large defects in peptidyl-transfer, but instead may result from ribosomes that become effectively inactivated (e.g. as a result of complex instability on homopolymeric A messages, etc). Whatever the cause for an initial ribosome pausing event on iterated AAA sequences, the ribosome can either slide or perform another round of peptide bond formation. If the ribosome slides such that another AAA codon is positioned in the A site, the next step will also be slow, while if sliding somehow positions a non-lysine codon in the A site, recovery from slow elongation may occur. In our *in vitro* system translating di-lysine messages, we are able to observe sliding when consecutive AAA-codons are present because we force a strong pause after MKK formation by leaving out downstream factors required for translation to proceed (Figure 3). Our data suggest that ribosome sliding on iterated AAA sequences is the major difference between the translation of poly(AAA)- and poly(AAG)-containing messages that results in substantially different protein outputs. While each sequential addition of lysine in an iterated AAG sequence may be slow, the ribosome maintains frame and ultimately is able to produce full-length protein. By contrast, with repeated AAA sequences, the ribosome can eventually escape the homopolymeric A sequence through repeated sliding events, often emerging out-of-frame from the A stretch, and thus unable to produce full-length protein.

Ribosome sliding on poly(A) is distinct from traditional programmed ribosomal movements such as +1 (Farabaugh and Bjork 1999; Taliaferro and Farabaugh 2007) and -1 frame-shifts (Plant et al. 2003; Caliskan et al. 2014; Chen et al. 2014; Kim et al. 2014; Dinman et al. 1991). During a programmed frame-shifting (PRF) event, specific signals direct elongating ribosomes to shift reading frame by one base in the 5’ (-1) or 3’ (+1) direction (Dinman 2012). -1

PRFs signals are typically characterized by a 'slippery' sequence (X XXY YYZ) that is modulated by the presence of a downstream secondary structure, most commonly a pseudoknot (Plant et al. 2003; Jacobs et al. 2007; Caliskan et al. 2014; Chen et al. 2014; Kim et al. 2014). The secondary structure impairs the normal movement of the ribosome during translocation, and promotes the frame-shift event in an EF-G dependent manner (Caliskan et al. 2014; Chen et al. 2014). +1 PRFs signals are more diverse than -1 PRFs, but still generally depend on a slippery sequence and a downstream element (e.g. secondary structure or rare codon) that causes the ribosome to pause (Dinman 2012). Iterated A stretches are inherently slippery and contain a built-in translation pause (adding consecutive lysines is slow – Figure 2), however the poly(A) sequences that we have studied lack significant secondary structure downstream that might contribute to limiting unregulated ribosome sliding. As such, when ribosomes slide on iterated AAA codons, forward and backward movements may be permitted. The scale of the movements undergone during a ribosome sliding event may be more similar to those documented in translational bypassing on the gene product 60 of bacteriophage T4 which is synthesized from a discontinuous reading frame (Samatova et al. 2014). Importantly, however, in contrast to this specific concerted large-scale movement (50 nucleotides) which results in the production of a single peptide product, ribosome sliding is different in that no single outcome appears to be encoded by the event. The inability of the ribosome to translate a discrete product on homopolymeric A sequences likely explains the bioinformatic analyses demonstrating that poly(A) sequences are strongly selected against in coding sequences containing iterated lysines (Table 1). Consistent with this idea, in *E. coli* we find that the minimum length (11) of a homopolymeric A sequence needed to trigger ribosome sliding in the

PURE cell free translation system (Figure 5, and Figure 5- figure supplement 1) correlates with the length of lysine stretch at which homopolymeric sequences are selected against in mRNA coding regions (Table 1).

There are multiple reports in the literature indicating that frame-shifted ribosomes can trigger NMD (Belew et al. 2011; Belew et al. 2014). We find that mRNA levels for reporters containing $(AAA)_{12}$ or $(AAGAAGAAA)_4$, but not $(AAG)_{12}$ sequences, are reduced in a Upf1-dependent manner. These data are consistent with the idea that sliding on homopolymeric A stretches can eventually lead to ribosomes reaching out-of-frame premature termination codons (Figure 6). A recent report in the literature argued that translation of poly-lysine stretches led to an unusual termination event on a sense codon (AAA or AAG) mediated by eRF3 (presumably in concert with its binding partner eRF1) (Chiabudini et al. 2014). These observations bring to mind premature termination events on sense codons documented in *E. coli* (Zaher and Green 2009); this quality control system was proposed to increase the fidelity of translation by minimizing frame-shifting and eliminating errors made during tRNA selection. We note that the premature termination event that we previously documented in *E. coli* was highly dependent on RF3, while the termination event documented in *E. coli* in this manuscript at homopolymeric A sequences is RF3-independent (Figure 4 – figure supplement 1). Given the clear evidence that we provide for ribosome sliding in the *E. coli* system and the inability to observe eRF1:eRF3-mediated peptide release on homopolymeric A programmed yeast ribosome complexes *in vitro* (Figure 6 – figure supplement 2), we suggest that the most likely explanation for the eRF3-dependent truncated product generated in yeast cells on $(AAGAAGAAA)_4$–encoding reporters in Chiabudini et al. is the result of ribosome sliding and

canonical recognition of downstream premature stop codons. We note that there are multiple out-of-frame stop codons following the $(AAGAAGAAA)_4$-repeat that could account for the observed products in Chiabudini et al (Chiabudini et al. 2014).

We were intrigued by the observation that the $(AAGAAGAAA)_4$ reporter mRNA levels are more efficiently recovered than those of the $(AAA)_{12}$ reporter mRNA in a *UPF1*-deletion strain. We speculate that the more modest sliding within the (AAGAAGAAA)-repeats might be distinguished from the sliding on (AAA)-repeats in an important way. Sliding within homopolymeric AAA sequence most typically results in another nearby AAA codon being poised in the A site, and another inefficient elongation event with Lys-$tRNA^{Lys}$. Ribosomes that eventually exit the polyA sequence to reach heteropolymeric sequence and an out-of-frame downstream premature stop codon will trigger NMD; ribosomes that struggle to get past the very long stretch of iterated lysine codons will instead trigger NSD. As such, the mRNA levels for the $(AAA)_{12}$ reporter are partially recovered by a *UPF1* deletion and partially recovered by a *DOM34* deletion (data not shown). By contrast, on the (AAGAAGAAA)-repeat reporters, sliding has the potential to quickly place the ribosomes in a more productive frame for efficient elongation (one frame will result in Arg-Arg-Lys (RRK) repeats while the other frame will result in Glu-Glu-Lys (EEK) repeats). While we might predict that the poly(basic) RRKRRKRRKRR peptide will also be slowly translated, a ribosome that slides into the frame encoding the EEKEEKEEKEE peptide should be able to resume efficient elongation. As such, fewer ribosomes may trigger NSD and, instead, a majority of ribosomes will reach downstream premature stop codons that trigger NMD. These ideas can easily be understood in the context of the model in Figure 7 where differences in the elongation rates (e.g. slow for iterated lysine residues but fast

412 for incorporation of other amino acids) will impact the relative contribution of ribosome sliding
413 to overall outcome.

414 NSD was originally identified by following the degradation of transcripts lacking
415 termination codons (Frischmeyer et al. 2002; van Hoof et al. 2002). These studies led to the
416 idea that NSD is triggered when the ribosome stalls while translating a poly(basic) lysine
417 sequence. NSD is commonly studied using reporters in yeast that contain poly(basic) inserts;
418 common lysine and arginine inserts that have been investigated include $(AAA)_{12}$, $(AAG)_{12}$, (AAG-
419 AAG-AAA)$_4$, and (CGG-$(CGA)_2$-CGG-$(CGC)_2$)$_2$ (Ito-Harashima et al. 2007; Dimitrova et al. 2009;
420 Bengtson and Joazeiro 2010; Brandman et al. 2012; Chiabudini et al. 2012; Chiabudini et al.
421 2014). Consistent with our findings, previous studies reported differences in protein output in
422 yeast when these different sequences are translated (Ito-Harashima et al. 2007; Dimitrova et al.
423 2009); iterated AAA codons are more detrimental to overall expression than iterated AAG
424 codons. Despite these differences, because the mRNA and protein levels for all of these are
425 broadly sensitive to known NSD factors (Ltn1, Dom34, Ski7), poly(basic) sequences have been
426 treated equally. Our results demonstrating that ribosomes can slide on consecutive AAA codons
427 suggest that there may be important distinctions to be made in considering these reporters and
428 that there may be substantial mechanistic overlaps in these systems.

429 Even though cells rarely maintain homopolymeric A sequences in ORFs, there are some
430 situations where the ribosome likely must deal with homopolymeric A stretches in both
431 bacteria and eukaryotes. In bacteria, mRNAs are typically polyadenylated as part of the normal
432 decay process (Dreyfus and Regnier 2002). For example, ribosome sliding might provide an

433 escape for ribosomes already engaged on these mRNAs (a form of ribosome rescue). In
434 eukaryotes, virtually all mRNAs in the cell are polyadenylated, but usually a stop codon is found
435 at the end of the encoded ORF. However, there is abundant recent evidence indicating that a
436 significant portion of yeast (14%) and human (9%) genes contain at least one alternative
437 polyadenylation site within their coding sequence (Ozsolak et al. 2010). It has even been
438 suggested that premature polyadenylation may become up-regulated in cancerous cells (Berg
439 et al. 2012). In cases where premature polyadenylation takes place within the ORF, the
440 ribosome will surely encounter a homopolymeric A sequence, likely triggering so called Non-
441 Stop-Decay (NSD). In light of the results presented here, we would suggest that the triggering of
442 NSD (and associated mRNA decay, proteolysis and ribosome recycling) occurs following the
443 slow translation of iterated lysines and ribosome sliding events. The ubiquity of premature
444 polyadenylation suggests that NSD broadly serves as an important pathway for regulating gene
445 expression. The observation of synonymous AAG to AAA changes in iterated lysine stretches in
446 genes upregulated in cancer provides support for the significance of this mechanism of gene
447 regulation (Arthur et al. 2014). The widespread use of polyadenylation for non-coding purposes
448 in mRNA transcripts may find its origins in the inability of the decoding machine, the ribosome,
449 to carefully control the behavior of these sequences.

450

451

## Materials and methods

### Reporter creation

The Thrdx-HA-mCherry (Figure 1A, Supplementary File 1) no insert reporter expressed in *E. coli* and the PURExpress cell free translation system was created using Gateway cloning to include the 2HA-mCherry sequence in the pBAD-DEST49 vector. The vectors containing inserts (Thrdx-HA-insert-mCherry: $(AAA)_{12}$, $(AAA)_6$, $(AAG)_{12}$, $(AAGAAGAAA)_4$, $(GAA)_{12}$, TAA (STOP), $(A)_{9\text{-}13}$, etc) were subsequently derived from this clone. To create the mCherry reporter expressed in yeast (Figure 1A), the Thrdx-HA-mCherry and Thrdx-HA-insert-mCherry sequences were amplified out of the pBAD-DEST49 vectors and cloned into the p-ENTR/D-TOPO vector. The vector was then reacted with lr-clonease II to move the sequences into the pYES-DEST52 plasmid. The dual luciferase reporter described in Figure 1A was based on the dual luciferase plasmid from Takacs et al (Takacs et al. 2011). In this reporter, Renilla and Firefly luciferase are under the control of ADH and GPD promoters, respectively. We inserted sequences of interest into the N-terminus of *Renilla* luciferase .

### *In vivo* protein expression and visualization

Thrdx-HA-mCherry and Thrdx-HA-insert-mCherry constructs were expressed in 6 mL *E. coli* grown in LB-Ampicillin. The cells were grown to an OD of 0.4-0.6, induced with 25 µL of 5g/10mL arabinose, then harvested 2 hours post-induction. In yeast, the Thrdx-HA-mCherry constructs were expressed in wild-type and *upf1*Δ *S. cerevisiae* (BY4741) grown in 5mL of –URA/+galactose media to an OD of 0.6. The dual luciferase reporters were transformed into yeast and grown in –URA/+glucose media, and harvested at an OD of 0.6. Proteins production

was analyzed via fluorescence, luminescence (Figure 1) or western blot analysis (Figure 4 – figure supplement 2).

**Assessing lysine incorporation in fully reconstituted *in vitro* translation assays**

70S initiation complexes (ICs) were prepared using *E. coli* ribosomes programmed with various mRNAs and f-[$^{35}$S]-Met-tRNA$^{Met}$ in the P site. mRNAs were generated by transcription with T7 polymerase and ICs were formed, pelleted, and resuspended as previously described (Youngman et al. 2004) on our messages of interest. Translation assays were initiated when equal volumes of ternary complex (10-20 μM charged tRNA, 12 μM EFG, 60 μM EfTu) were added to 0.2 nM 70S initiation complexes. Assays were performed in 219-Tris buffer (50 mM Tris pH 7.5, 70 mM $NH_4Cl$, 30 mM KCl, 7 mM $MgCl_2$, 5 mM βME). The limited addition of iterated lysines on a $MK_{A5}$-STOP message was also observed in polymix buffer (50 mM $K_2HPO4$ pH 7.5, 95 mM KCl, 5 mM $NH_4Cl$, 5 mM $Mg(OAc)_2$, 0.5 mM $CaCl_2$, 8 mM putrescine, 1 mM spermidine, 1 mM DTT). To measure the rates of amino acid incorporation, the reactions are quenched with 500 mM KOH (final concentration) at discrete time points (0 seconds – 30 minutes) either by hand or on a quench-flow apparatus. For assays including release factors for the duration of the reaction (Figure 3C), RF1 and additional GTP were added prior to the initiation of translation (final concentrations 1μM and 200 μM, respectively). The time-points were diluted 1:10 in nuclease free water and the reactants, intermediates and products visualized by electrophoretic TLC, as previously described (Zaher and Green 2009). The reactants, products and intermediates were visualized by phosophorimaging and quantified

493 with ImageQuant. The kinetic fits were modeled using Mathematica (details in Figure 2 – figure
494 supplement 2).

495 **Expression of reporters in the PURExpress *in vitro* translation system**

496 The Thrdx-HA-mCherry and Thrdx-HA-insert-mCherry reporters were expressed in the
497 PURExpress *in vitro* translation system (NEB) from PCR products. The peptidyl-tRNA construct
498 was generated by creating a truncated mRNA lacking a stop codon directly after the Thrdx-HA
499 sequence. The PURExpress reactions were initiated by mixing 1 µL of PCR product (29 – 22
500 ng/uL), 2 µL of solution A, 1.5 µL of solution B, and 0.6 µL of $^{35}$S-methionine. The reactions were
501 run for 45-60 minutes at 37$^{o}$C. Following translation, the products were immediately heat-
502 denatured and loaded on a 4-12% Bis-Tris gel at 4$^{o}$C in XT-MES buffer. For the experiments in
503 which the PURExpress reaction products were treated with RNase A (Figure 4B), 0.5-1 µg of
504 RNase A (Ambion) was added to each reaction and solutions were incubated on ice for an
505 additional 30 minutes before being denatured and loaded on a gel. The peptide products of the
506 PURExpress reactions were visualized by Phosphoimager and quantified with ImageQuant
507 (Figure 3 – figure supplement 2, and Figure 5 – figure supplement 1).

508 **Toeprinting assays**

509 DNA templates were PCR amplified from plasmids (PCR-Blunt II-TOPO vector) encoding
510 MEA(INSERT)EAEDYKDD sequences. The PURExpress cell-free transcription-translation system
511 (NEB) was used for *in vitro* protein synthesis. Reactions were run for 30 minutes at 37$^{o}$C by
512 mixing 0.2-pmol of DNA template, 2.5 µl of Solution A and 1 µl of Solution B along with either
513 0.5 µl of DMSO (5%) or thiostrepton (0.5 mm in 5% DMSO). 1 pmol of $^{32P}$ATP-labeled NV1

primer was added, and reverse transcription was performed with AMV as previously described (Vazquez-Laslop et al. 2008; Tanner et al. 2009). Reactions were phenol and chloroform extracted, ethanol precipitated and visualized on a 6% denaturing PAGE gel. Sequencing lanes were generated from plasmids using the Sequenase 2.0 DNA sequencing kit (Affymetrix). All bands were visualized by PhosphorImager.

**Real-time quantitative reverse transcription PCR (qRT PCR) to measure reporter mRNA levels**

Reporter mRNA levels were quantified by qRT-PCR using the iQ5 iCycler system (Bio-Rad) and iQ SYBR Green Supermix (Bio-Rad).

**Measuring mRNA decay**

To measure the rate of mRNA decay in yeast for our mCherry reporters, we grew wild-type and *upf1*Δ cells expressing reporters in –ura/galactose media at 30$^{o}$C to an OD600 of 0.4. Cells were washed three times with –ura media lacking sugar, then re-suspended in -ura/glucose media; the transcription of the reporter is shut-off by glucose. Samples were collected at discrete time points (0-90 minutes), and mRNA levels were analyzed by qRT PCR.

**Bioinformatic analyses**

*E. coli* K-12 substrain MG1655 complete genome, 4140 ORFs (data source: GenBank:U00096.3; http://www.ncbi.nlm.nih.gov/nuccore/U00096.3) and S. cerevisiae 5887 verified ORFs (data source: http://downloads.yeastgenome.org/sequence/S288C_reference/orf_protein/) have been used for extraction of lysine codon numbers and analyses of consecutive codons shown in Table 1.

Expected values for consecutive variants of lysine AAA and AAG codons were calculated based on observed values for a single AAA and AAG codons and their probabilities to be found in such arrangments. Observed values were calculated based on data from genomic distribution and total numbers of variants for two, three or four consecutive lys codons, respectively.

**Acknowledgements**

We would like to thank Slavica Pavlovic-Djuranovic and Risa Burr for help with materials, Jon Lorsch for sharing the dual luciferase plasmid (Takacs et al. 2011), and Allen Buskirk for reading. We would also like to thank the National Institutes of Health (R37 GM059425 to RG, and F32 GM100608 to KSK) for funding and the Howard Hughes Medical Foundation (RG) for salary support.

## References


Arenz S, Meydan S, Starosta AL, Berninghausen O, Beckmann R, Vazquez-Laslop N, Wilson DN. 2014. Drug Sensing by the Ribosome Induces Translational Arrest via Active Site Perturbation. *Molecular cell*.

Arthur L, Pavlovic-Djuranovic S, Koutmou KS, Green R, Szczesny P, Djuranovic S. 2014. Translational control by lysine coding A-rich sequences. *submitted*.

Belew AT, Advani VM, Dinman JD. 2011. Endogenous ribosomal frameshift signals operate as mRNA destabilizing elements through at least two molecular pathways in yeast. *Nucleic acids research* **39**: 2799-2808.

Belew AT, Meskauskas A, Musalgaonkar S, Advani VM, Sulima SO, Kasprzak WK, Shapiro BA, Dinman JD. 2014. Ribosomal frameshifting in the CCR5 mRNA is regulated by miRNAs and the NMD pathway. *Nature* **512**: 265-269.

Bengtson MH, Joazeiro CA. 2010. Role of a ribosome-associated E3 ubiquitin ligase in protein quality control. *Nature* **467**: 470-473.

Berg MG, Singh LN, Younis I, Liu Q, Pinto AM, Kaida D, Zhang Z, Cho S, Sherrill-Mix S, Wan L et al. 2012. U1 snRNP determines mRNA length and regulates isoform expression. *Cell* **150**: 53-64.

Bhushan S, Hoffmann T, Seidelt B, Frauenfeld J, Mielke T, Berninghausen O, Wilson DN, Beckmann R. 2011. SecM-stalled ribosomes adopt an altered geometry at the peptidyl transferase center. *PLoS Biol* **9**: e1000581.

566 Brandman O, Stewart-Ornstein J, Wong D, Larson A, Williams CC, Li GW, Zhou S, King D, Shen
567 PS, Weibezahn J et al. 2012. A ribosome-bound quality control complex triggers
568 degradation of nascent peptides and signals translation stress. *Cell* **151**: 1042-1054.
569 Caliskan N, Katunin VI, Belardinelli R, Peske F, Rodnina MV. 2014. Programmed -1 frameshifting
570 by kinetic partitioning during impeded translocation. *Cell* **157**: 1619-1631.
571 Chan PP, Lowe TM. 2009. GtRNAdb: a database of transfer RNA genes detected in genomic
572 sequence. *Nucleic acids research* **37**: D93-97.
573 Chen J, Petrov A, Johansson M, Tsai A, O'Leary SE, Puglisi JD. 2014. Dynamic pathways of -1
574 translational frameshifting. *Nature* **512**: 328-332.
575 Chiabudini M, Conz C, Reckmann F, Rospert S. 2012. Ribosome-associated complex and Ssb are
576 required for translational repression induced by polylysine segments within nascent
577 chains. *Molecular and cellular biology* **32**: 4769-4779.
578 Chiabudini M, Tais A, Zhang Y, Hayashi S, Wolfle T, Fitzke E, Rospert S. 2014. Release Factor
579 eRF3 Mediates Premature Translation Termination on Polylysine-Stalled Ribosomes in
580 Saccharomyces cerevisiae. *Molecular and cellular biology* **34**: 4062-4076.
581 Cochella L, Green R. 2005. An active role for tRNA in decoding beyond codon:anticodon pairing.
582 *Science* **308**: 1178-1180.
583 Dimitrova LN, Kuroha K, Tatematsu T, Inada T. 2009. Nascent peptide-dependent translation
584 arrest leads to Not4p-mediated protein degradation by the proteasome. *The Journal of*
585 *biological chemistry* **284**: 10343-10352.
586 Dinman JD. 2012. Mechanisms and implications of programmed translational frameshifting.
587 *Wiley interdisciplinary reviews RNA* **3**: 661-673.

588 Dinman JD, Icho T, Wickner RB. 1991. A -1 ribosomal frameshift in a double-stranded RNA virus
589 of yeast forms a gag-pol fusion protein. *Proceedings of the National Academy of*
590 *Sciences of the United States of America* **88**: 174-178.
591 Doerfel LK, Wohlgemuth I, Kothe C, Peske F, Urlaub H, Rodnina MV. 2013. EF-P is essential for
592 rapid synthesis of proteins containing consecutive proline residues. *Science* **339**: 85-88.
593 Doma MK, Parker R. 2006. Endonucleolytic cleavage of eukaryotic mRNAs with stalls in
594 translation elongation. *Nature* **440**: 561-564.
595 Dreyfus M, Regnier P. 2002. The poly(A) tail of mRNAs: bodyguard in eukaryotes, scavenger in
596 bacteria. *Cell* **111**: 611-613.
597 Farabaugh PJ, Bjork GR. 1999. How translational accuracy influences reading frame
598 maintenance. *The EMBO journal* **18**: 1427-1434.
599 Frischmeyer PA, van Hoof A, O'Donnell K, Guerrerio AL, Parker R, Dietz HC. 2002. An mRNA
600 surveillance mechanism that eliminates transcripts lacking termination codons. *Science*
601 **295**: 2258-2261.
602 Gong F, Yanofsky C. 2002. Instruction of translating ribosome by nascent peptide. *Science* **297**:
603 1864-1867.
604 Gromadski KB, Daviter T, Rodnina MV. 2006. A uniform response to mismatches in codon-
605 anticodon complexes ensures ribosomal fidelity. *Molecular cell* **21**: 369-377.
606 Gutierrez E, Shin BS, Woolstenhulme CJ, Kim JR, Saini P, Buskirk AR, Dever TE. 2013. eIF5A
607 promotes translation of polyproline motifs. *Molecular cell* **51**: 35-45.
608 Ito K, Chiba S. 2013. Arrest peptides: cis-acting modulators of translation. *Annu Rev Biochem* **82**:
609 171-202.

610 Ito-Harashima S, Kuroha K, Tatematsu T, Inada T. 2007. Translation of the poly(A) tail plays
611 crucial roles in nonstop mRNA surveillance via translation repression and protein
612 destabilization by proteasome in yeast. *Genes Dev* **21**: 519-524.
613 Izawa T, Tsuboi T, Kuroha K, Inada T, Nishikawa S, Endo T. 2012. Roles of dom34:hbs1 in
614 nonstop protein clearance from translocators for normal organelle protein influx. *Cell*
615 *reports* **2**: 447-453.
616 Jacobs JL, Belew AT, Rakauskaite R, Dinman JD. 2007. Identification of functional, endogenous
617 programmed -1 ribosomal frameshift signals in the genome of Saccharomyces
618 cerevisiae. *Nucleic acids research* **35**: 165-174.
619 Kim HK, Liu F, Fei J, Bustamante C, Gonzalez RL, Jr., Tinoco I, Jr. 2014. A frameshifting
620 stimulatory stem loop destabilizes the hybrid state and impedes ribosomal
621 translocation. *Proceedings of the National Academy of Sciences of the United States of*
622 *America* **111**: 5538-5543.
623 Klauer AA, van Hoof A. 2012. Degradation of mRNAs that lack a stop codon: a decade of
624 nonstop progress. *Wiley interdisciplinary reviews RNA* **3**: 649-660.
625 Kuroha K, Akamatsu M, Dimitrova L, Ito T, Kato Y, Shirahige K, Inada T. 2010. Receptor for
626 activated C kinase 1 stimulates nascent polypeptide-dependent translation arrest.
627 *EMBO reports* **11**: 956-961.
628 Lu J, Deutsch C. 2008. Electrostatics in the ribosomal tunnel modulate chain elongation rates.
629 *Journal of molecular biology* **384**: 73-86.
630 Nakatogawa H, Ito K. 2002. The ribosomal exit tunnel functions as a discriminating gate. *Cell*
631 **108**: 629-636.

632 Ozsolak F, Kapranov P, Foissac S, Kim SW, Fishilevich E, Monaghan AP, John B, Milos PM. 2010.
633 Comprehensive polyadenylation site maps in yeast and human reveal pervasive
634 alternative polyadenylation. *Cell* **143**: 1018-1029.
635 Plant EP, Jacobs KL, Harger JW, Meskauskas A, Jacobs JL, Baxter JL, Petrov AN, Dinman JD. 2003.
636 The 9-A solution: how mRNA pseudoknots promote efficient programmed -1 ribosomal
637 frameshifting. *Rna* **9**: 168-174.
638 Ratinier M, Boulant S, Combet C, Targett-Adams P, McLauchlan J, Lavergne JP. 2008.
639 Transcriptional slippage prompts recoding in alternate reading frames in the hepatitis C
640 virus (HCV) core sequence from strain HCV-1. *J Gen Virol* **89**: 1569-1578.
641 Samatova E, Konevega AL, Wills NM, Atkins JF, Rodnina MV. 2014. High-efficiency translational
642 bypassing of non-coding nucleotides specified by mRNA structure and nascent peptide.
643 *Nature communications* **5**: 4459.
644 Seidelt B, Innis CA, Wilson DN, Gartmann M, Armache JP, Villa E, Trabuco LG, Becker T, Mielke
645 T, Schulten K et al. 2009. Structural insight into nascent polypeptide chain-mediated
646 translational stalling. *Science* **326**: 1412-1415.
647 Shoemaker CJ, Eyler DE, Green R. 2010. Dom34:Hbs1 promotes subunit dissociation and
648 peptidyl-tRNA drop-off to initiate no-go decay. *Science* **330**: 369-372.
649 Shoemaker CJ, Green R. 2012. Translation drives mRNA quality control. *Nature structural &*
650 *molecular biology* **19**: 594-601.
651 Takacs JE, Neary TB, Ingolia NT, Saini AK, Martin-Marcos P, Pelletier J, Hinnebusch AG, Lorsch
652 JR. 2011. Identification of compounds that decrease the fidelity of start codon
653 recognition by the eukaryotic translational machinery. *Rna* **17**: 439-452.

654 Taliaferro D, Farabaugh PJ. 2007. An mRNA sequence derived from the yeast EST3 gene
655 stimulates programmed +1 translational frameshifting. *Rna* **13**: 606-613.
656 Tanner DR, Cariello DA, Woolstenhulme CJ, Broadbent MA, Buskirk AR. 2009. Genetic
657 identification of nascent peptides that induce ribosome stalling. *The Journal of biological*
658 *chemistry* **284**: 34809-34818.
659 Tsuboi T, Kuroha K, Kudo K, Makino S, Inoue E, Kashima I, Inada T. 2012. Dom34:hbs1 plays a
660 general role in quality-control systems by dissociation of a stalled ribosome at the 3' end
661 of aberrant mRNA. *Molecular cell* **46**: 518-529.
662 Tsuchihashi Z, Brown PO. 1992. Sequence requirements for efficient translational frameshifting
663 in the Escherichia coli dnaX gene and the role of an unstable interaction between
664 tRNA(Lys) and an AAG lysine codon. *Genes Dev* **6**: 511-519.
665 Ude S, Lassak J, Starosta AL, Kraxenberger T, Wilson DN, Jung K. 2013. Translation elongation
666 factor EF-P alleviates ribosome stalling at polyproline stretches. *Science* **339**: 82-85.
667 van Hoof A, Frischmeyer PA, Dietz HC, Parker R. 2002. Exosome-mediated recognition and
668 degradation of mRNAs lacking a termination codon. *Science* **295**: 2262-2264.
669 Vazquez-Laslop N, Thum C, Mankin AS. 2008. Molecular mechanism of drug-dependent
670 ribosome stalling. *Molecular cell* **30**: 190-202.
671 Woolstenhulme CJ, Parajuli S, Healey DW, Valverde DP, Petersen EN, Starosta AL, Guydosh NR,
672 Johnson WE, Wilson DN, Buskirk AR. 2013. Nascent peptides that block protein synthesis
673 in bacteria. *Proceedings of the National Academy of Sciences of the United States of*
674 *America* **110**: E878-887.

675 Youngman EM, Brunelle JL, Kochaniak AB, Green R. 2004. The active site of the ribosome is
676 composed of two layers of conserved nucleotides with distinct roles in peptide bond
677 formation and peptide release. *Cell* **117**: 589-599.
678 Zaher HS, Green R. 2009. Quality control by the ribosome following peptide bond formation.
679 *Nature* **457**: 161-166.

680

681

## Tables and legends

### Table 1.

| Organism | Sequence | Occurances | Fraction observed | Fraction expected | Enrichment |
|---|---|---|---|---|---|
| *E. coli* | AAG-AAG | 244 | 0.08 | 0.08 | 1.01 |
| | AAG-AAA | 902 | 0.29 | 0.20 | 1.45 |
| | AAA-AAG | 544 | 0.18 | 0.20 | 0.87 |
| | AAA-AAA | 1416 | 0.46 | 0.52 | 0.88 |
| | AAG-AAG-AAG | 9 | 0.07 | 0.02 | 3.37 |
| | AAG-AAG-AAA | 20 | 0.16 | 0.06 | 2.89 |
| | AAG-AAA-AAG | 21 | 0.17 | 0.06 | 3.03 |
| | AAA-AAG-AAG | 4 | 0.03 | 0.06 | 0.58 |
| | AAG-AAA-AAA | 36 | 0.29 | 0.14 | 2.00 |
| | AAA-AAG-AAA | 29 | 0.23 | 0.14 | 1.61 |
| | AAA-AAA-AAG | 4 | 0.03 | 0.14 | 0.22 |
| | AAA-AAA-AAA | 1 | 0.01 | 0.38 | 0.02 |
| | AAG-AAG-AAA-AAG | 1 | 0.25 | 0.02 | 16.07 |
| | AAG-AAG-AAA-AAA | 1 | 0.25 | 0.04 | 6.20 |
| | AAA-AAG-AAA-AAA | 2 | 0.50 | 0.10 | 4.78 |
| *S. cerevisiae* | AAG-AAG | 3845 | 0.21 | 0.14 | 1.45 |
| | AAG-AAA | 5183 | 0.28 | 0.24 | 1.20 |
| | AAA-AAG | 4505 | 0.24 | 0.24 | 1.04 |
| | AAA-AAA | 4858 | 0.26 | 0.39 | 0.69 |
| | AAG-AAG-AAG | 261 | 0.16 | 0.05 | 2.87 |
| | AAG-AAG-AAA | 234 | 0.14 | 0.09 | 1.57 |
| | AAG-AAA-AAG | 224 | 0.13 | 0.09 | 1.51 |
| | AAA-AAG-AAG | 189 | 0.11 | 0.09 | 1.27 |
| | AAG-AAA-AAA | 211 | 0.13 | 0.15 | 0.87 |
| | AAA-AAG-AAA | 261 | 0.16 | 0.15 | 1.07 |
| | AAA-AAA-AAG | 117 | 0.07 | 0.15 | 0.48 |
| | AAA-AAA-AAA | 171 | 0.10 | 0.24 | 0.43 |
| | AAG-AAG-AAG-AAG | 24 | 0.10 | 0.02 | 4.88 |
| | AAA-AAG-AAG-AAG | 28 | 0.12 | 0.03 | 3.48 |
| | AAG-AAA-AAG-AAG | 23 | 0.10 | 0.03 | 2.86 |
| | AAG-AAG-AAA-AAG | 19 | 0.08 | 0.03 | 2.36 |
| | AAG-AAG-AAG-AAA | 27 | 0.11 | 0.03 | 3.35 |
| | AAG-AAG-AAA-AAA | 13 | 0.05 | 0.06 | 0.99 |
| | AAG-AAA-AAG-AAA | 19 | 0.08 | 0.06 | 1.44 |
| | AAA-AAG-AAG-AAA | 11 | 0.05 | 0.06 | 0.83 |
| | AAA-AAG-AAA-AAG | 17 | 0.07 | 0.06 | 1.29 |
| | AAG-AAA-AAA-AAG | 5 | 0.02 | 0.06 | 0.38 |
| | AAA-AAA-AAG-AAG | 9 | 0.04 | 0.06 | 0.68 |
| | AAG-AAA-AAA-AAA | 9 | 0.04 | 0.09 | 0.42 |
| | AAA-AAG-AAA-AAA | 14 | 0.06 | 0.09 | 0.65 |
| | AAA-AAA-AAG-AAA | 6 | 0.03 | 0.09 | 0.28 |
| | AAA-AAA-AAA-AAG | 5 | 0.02 | 0.09 | 0.23 |
| | AAA-AAA-AAA-AAA | 9 | 0.04 | 0.15 | 0.25 |

**Table 1. Bioinformatic analyses of poly(lysine) sequences.** The prevalence precise sequences encoding 2-3 consecutive lysine residues in *E. coli* and *S. cerevisiae* are displayed. The raw

686 number of ‘occurrences’ are listed for each sequence. The enrichment values listed reflect the

687 fraction observed / fraction expected.

688

689 **Figures titles and legends**

690 **Figure 1. Protein production is differentially diminished by iterated lysine codons (AAA vs.**
691 **AAG) in *E. coli* and *S. cerevisiae*. (A)** Schematics of the mCherry (top) and luciferase (bottom)
692 reporters used in this study. The mCherry reporter contains an N-terminal thioredoxin (Thrdx)
693 domain, 3HA-tag, sequence of interest (black section), followed by the C-terminal mCherry
694 sequence. The luciferase reporter includes sequences of interest at the N-terminal end of
695 Renilla. Firefly is used in this construct as an internal control. **(B)** Relative amounts of protein
696 expressed from reporters expressed in *E. coli* (mCherry, red) and *S. cerevisiae* (luciferase,
697 green). Error bars results from for the standard error of at least three experiments.

698

699 **Figure 2. Kinetic defect observed on addition of 2$^{nd}$ and 3$^{rd}$ lysine residues in iterated lysine**
700 **stretch. (A)** Example TLC displaying the *E. coli* translation products of a AUG-$(AAA)_5$-UAA
701 message. The +/- poles of the electrophoretic TLC are indicated. $MK_4$ and $MK_5$ products (and
702 those with greater numbers of lysine) are difficult to resolve in this system but the other
703 products are easily visualized. (**B)** Kinetic scheme for rate constants of sequential lysine
704 additions to peptide chain. **(C)** Bar graph displaying rate constants for the addition of individual
705 lysines to a variety of messages: MKFK-Stop (gray), $MK_{A5}$-Stop (blue), $MK_{G5}$-Stop (black), and
706 MFK (gray).

707

**Figure 3. *E. coli* ribosomes add extra lysines on messages containing two sequential AAA, but not AAG, lysine codons. (A)** Illustration of the ribosome on the entire $MK_{A2}$-Stop message. **(B)** eTLCs showing the peptide products resulting from translation of indicated messages with Lys-$tRNA^{lys}$ (but no other tRNAs or release factors) present. **(C)** eTLC displaying the peptide products resulting from the translation of indicated messages in the presence of Lys-$tRNA^{Lys}$ alone, or in the presence of Lys-$tRNA^{Lys}$ + factors (either RF1 or Phe-$tRNA^{Phe}$) necessary for messages to be fully translated.

**Figure 4. Ribosomes 'slide' into new frame on poly(A)-containing messages in the PURE *in vitro* translation system. (A)** Expression of mCherry reporters (Figure 1A) in the *E. coli* PURE cell free translation system (NEB). The truncated band generated from the $(AAA)_{12}$ reporter is boxed in red. The expected sizes of the full-length, STOP protein and truncated reporter are 42 kDa, 15 kDa, and 17 kDa, respectively. **(B)** Expression of mCherry reporters in the PURE system and subsequent treatment of peptide products with RNase A. Only the positive control (with a truncated mRNA species) yielded a peptidyl-tRNA product that shifted in mobility upon RNase A treatment. **(C)** Expression of mCherry reporters (Fig. 1A) in the PURE *in vitro* translation system in the presence and absence of RFs (RFs = RF1, RF2, and RF3).

**Figure 5. Position and length of poly(A) stretch contributes to ribosome 'sliding' in the PURE *in vitro* translation system.** Expression of mCherry reporters containing poly(A) inserts of various lengths in the presence (+) and absence (-) of RFs.

**Figure 6. Deletion of Upf1p results in recovery of mRNA levels for poly(A) reporters in yeast.** Luciferase **(A)** and mCherry **(B)** reporters (Figure 1A) were expressed in wild-type and *upf1*Δ *S. cerevisiae,* and the levels of reporter RNA were quantified by qRT-PCR. Various insertions including 12 lysines ($(AAA)_{12}$, $(AAG)_{12}$, $(AAG_2AAA)_4$), stem-loop, or premature termination codon (PTC) in the coding sequence are specified on the x-axes.

**Figure 7. Model for events during ribosome sliding.** In this model translation is paused following the addition of the first lysine. The ribosome can than either slide or perform another round of peptide bond formation. If an AAA codon is positioned in the A site after sliding, the next step will also be slow, while if sliding results in a non-lysine codon in the A site, recovery from slow elongation may occur.

**Figure supplement titles and legends**

**Figure 2- figure supplement 1. Ribosomes stall while adding a second lysine.** Toeprinting assays were performed with constructs containing 1-12 consecutive lysines inserted (either AAG and AAA codons). Assays were performed in the presence and absence of thiostrepton to mark ribosomes on the initiating AUG codon. Sequences on which toe-prints appear are highlighted in red.

**Figure 2 – figure supplement 2. Modeling of rate constants in Mathematica. (A)** Kinetic scheme used to model the rate constants of sequential lysine additions to the peptide chain

751 (same as Figure 2A). We also attempted to model with peptidyl-tRNA drop-off rates included.
752 Inserting peptidyl-tRNA drop-off into our model decreases the quality of fits, and returns rates
753 of drop-off small enough that they are inconsequential relative to the time scale of the
754 reaction. **(B)** The top panel displays the differential equations used to solve for each rate
755 constant. The bottom panels display the mathematical solutions for the differential equations.
756 These solutions were used to perform modeling and fit the data. The fits were performed both
757 iteratively (e.g. we solved for $k_1$ by fitting the plots measuring the disappearance of M, then
758 input that value into the equation describing the appearance of MK to solve for $k_2$) and by
759 letting all of the values float for each data set. In both cases, the rate constants modeled were
760 essentially the same, indicating that the first lysine is added quickly ($k_1$), and subsequent lysines
761 ($k_2$, $k_3$) are added more slowly. **(C)** An example fit in Mathematica showing time course for the
762 formation and depletion of MK on a message with AAG codons. This time course, for example,
763 was used to model the $k_2$ value. **(D)** $R^2$ values for the fits for the appearance and disappearance
764 of each species used to model rate constants.

765

766 **Figure 3 – figure supplement 1. *E. coli* ribosomes add extra lysines to peptides translated on**
767 **messages containing sequential AAA-AAG lysine codons.** TLC showing all of the peptide
768 products resulting from translation of $MK_{A2}$V-Stop, $MK_{A3}$-Stop, $MK_{A4}$-STOP, and $MK_AK_GF$-Stop
769 messages with Lys-$tRNA^{lys}$ (but no other tRNAs or release factors) present.

770

**Figure 3 – figure supplement 2. Quantification of the percentage of translated peptide containing more lysine residues than expected.** Translation reactions were run in the presence of either Lys-tRNA$^{lys}$ only, or Lys-tRNA$^{lys}$ and other factors (Phe-tRNA$^{Phe}$ or RF1). All errors bars represent the standard error from at least three independent experiments.

**Figure 3 – figure supplement 3. T7 transcribed messages visualized on 15% denaturing PAGE gel**. **(A)** *In vitro* transcribed mRNAs used in our *in vitro* studies run as distinct, single bands on high-resolution denaturing PAGE gel. The RNA is visualized with methylene blue stain. **(B)** The mRNAs encoding consecutive AAA codons result in discrete length toeprint signatures, yielding specific bands corresponding to the full-length message on our toe-prints. We also performed RACE experiments on *in vitro* T7 transcribed mCherry reporter mRNAs containing $A_{18\text{-}36}$ sequences and found that with high frequency, our RNAs contained the expected number of As. Importantly, in both the cell free system and *in vivo*, T7 RNA polymerase is responsible for transcribing the mRNAs relevant to the output. Together, these data provide strong evidence that the mRNAs utilized throughout this study are accurately transcribed by T7 RNA polymerase.

**Figure 4 – figure supplement 1. Truncated product release is independent of RF3 in the PURExpress cell free translation system.** mCherry reporters (Figure 1A: no insert, $AAG_{12}$, $AAA_{12}$) were expressed in the PURExpress cell free translation system lacking release factors (RFs) (light gray). RFs were added back to the reactions individually (RF1 in green, RF2 in

purple), and in combination (RF1/3 in red and Rf2/3 dark gray). The plot displays the fraction of protein in the truncated band (100% x (radioactivity in truncated band / (radioactivity in truncated + full-length bands)).

**Figure 4 – figure supplement 2. Western blot (α-HA) of mCherry reporters (Figure 1A) expressed in *E. coli*.** The full-length peptide product is noted with the solid arrow, and the truncated band is highlighted with the dotted arrow. WT = no insert.

**Figure 5 – figure supplement 1. Quantification of the efficiency of ribosome sliding on mCherry reporters expressed in the PURExpress system.** mCherry reporters (Figure 1A: no insert, and various A stretches) were expressed in the PURExpress cell free translation system (Figure 5). The plot reports the percent of truncated peptide product expressed relative to total peptide product for each reporter (100% x (radioactivity in truncated band / (radioactivity in truncated + full-length bands)).

**Figure 6 – figure supplement 1. mRNA half-life of reporter containing iterated AAA codons is Upf1 dependent**. Representative experiments measuring the amount of mCherry reporter mRNA in wild-type BY4741 (black) and *upf1*Δ (blue) cells as a function of time following transcriptional shut-off for reporters containing **(A)** $(AAG)_{12}$, **(B)** $(AAA)_{12}$, and **(C)** $(AAG_2AAA)_4$ inserts. **(D)** The measured half-lives for decay of mCherry reporter mRNA in wild-type (BY4741) and *upf1*Δ cells.

**Figure 6 – figure supplement 2. eRF1:3 does not prematurely terminate translation on coding sequences in poly-lysine messages**. $MK_{A5}$-STOP message was translated with Lys-$tRNA^{Lys}$ present by *S. cerevisiae* ribosomes in a previously described yeast *in vitro* reconstituted system (Shoemaker, et al. 2010). The reaction was allowed to proceed for 10 minutes; aliquots of the reaction were quenched at various time points with KOH to hydrolyze the peptidyl-tRNA bond and allow for the visualization of discrete peptide products (right panel). After 10 minutes, eukaryotic release factors eRf1:eRF3 were added; time points quenched with formic acid; these lanes allow for visualization of peptides released from peptidyl-tRNA (shown in the left panel). Normally, eRF1:eRF3 should only catalyze the release of peptide products from ribosomes on stop codons. The release reaction was allowed to proceed for 5 minutes (left panel).

**Supplementary File 1. Primary sequence of mCherry with out of frame stop-codons highlighted.** The nucleotide sequence of the Thrdx-HA-mCherry reporters (Figure 1A) with all out of frame stop codons after the insertion site highlighted in yellow.

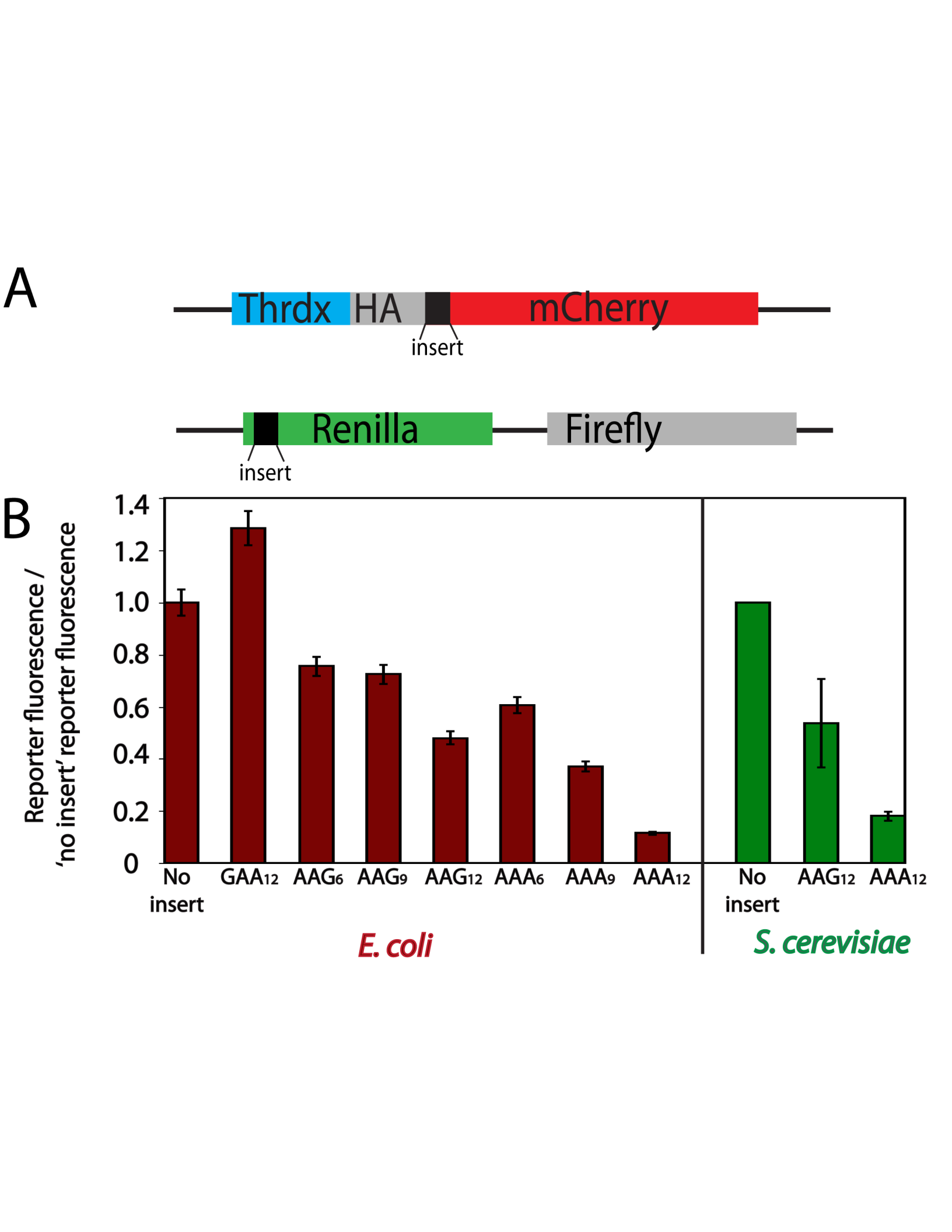
A
Thrdx
HA
mCherry
insert
Renilla
Firefly
insert
B
Reporter fluorescence /
'no insert' reporter fluorescence
1.4
1.2
1.0
0.8
0.6
0.4
0.2
0
No insert
GAA12
AAG6
AAG9
AAG12
AAA6
AAA9
AAA12
No insert
AAG12
AAA12
E. coli
S. cerevisiae

A

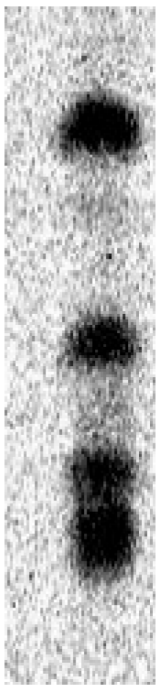
+
MK
MK2
MK3
MK4+
–

B

M + K
k1,obs
MK + K
k2,obs
MK2 + K
k3,obs
MK3 + K
k4,obs
k5,obs

C

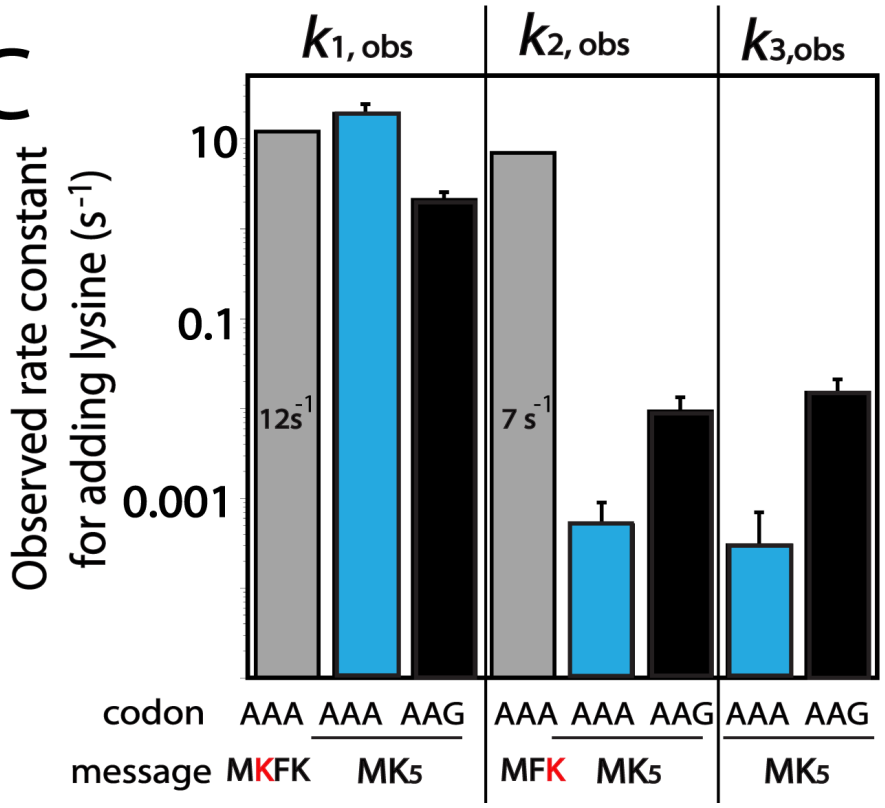
k1, obs
k2, obs
k3,obs
Observed rate constant for adding lysine (s-1)
10
0.1
0.001
12s-1
7 s-1
codon
AAA AAA AAG AAA AAA AAG AAA AAG
message
MKFK MK5 MFK MK5 MK5

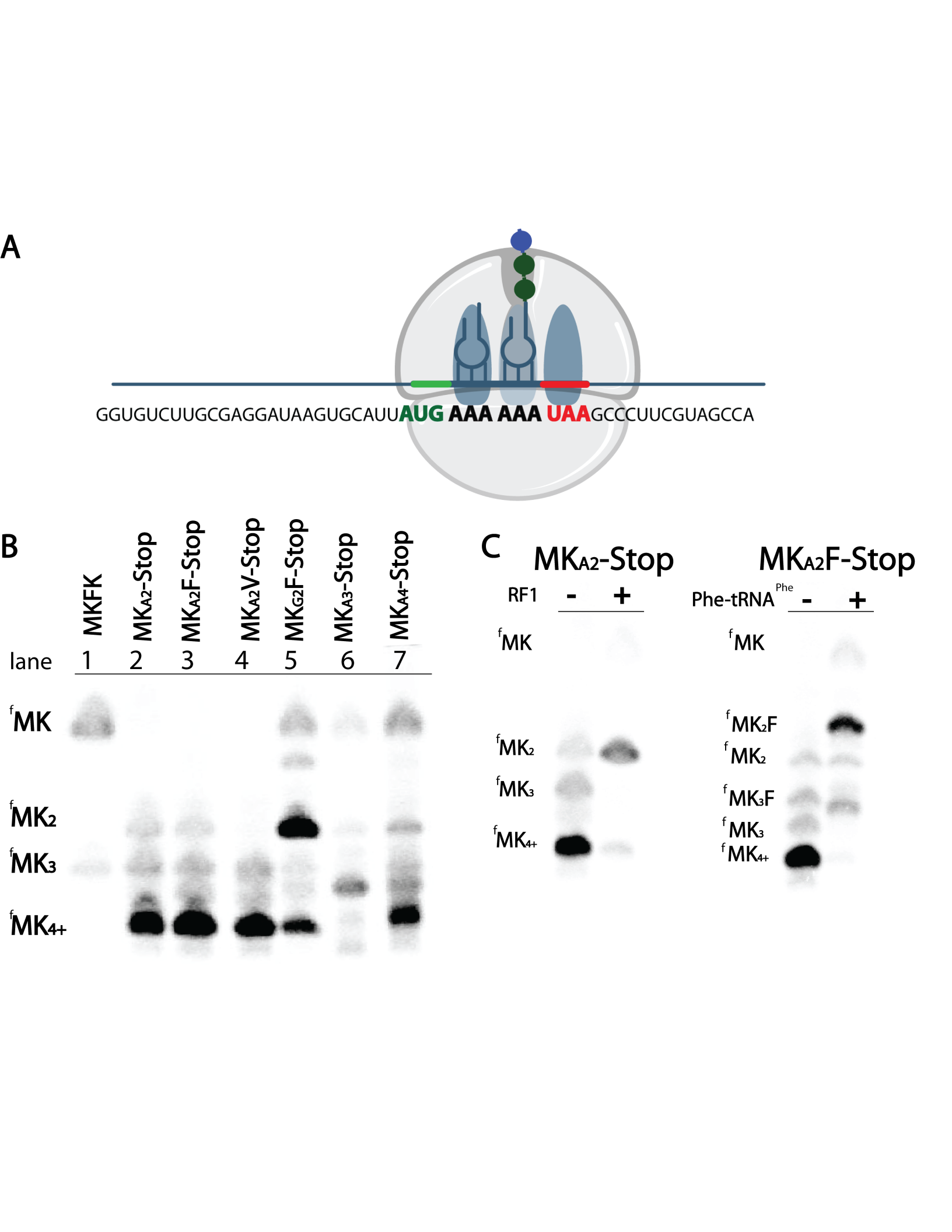
A
GGUGUCUUGCGAGGAUAAGUGCAUUAUG AAA AAA UAAGCCCUUCGUAGCCA
B
MKFK
MKA2-Stop
MKA2F-Stop
MKA2V-Stop
MKG2F-Stop
MKA3-Stop
MKA4-Stop
lane 1 2 3 4 5 6 7
fMK
fMK2
fMK3
fMK4+
C
MKA2-Stop
MKA2F-Stop
RF1 - +
Phe-tRNAPhe - +
fMK
fMK2
fMK3
fMK4+
fMK2F
fMK2
fMK3F
fMK3
fMK4+

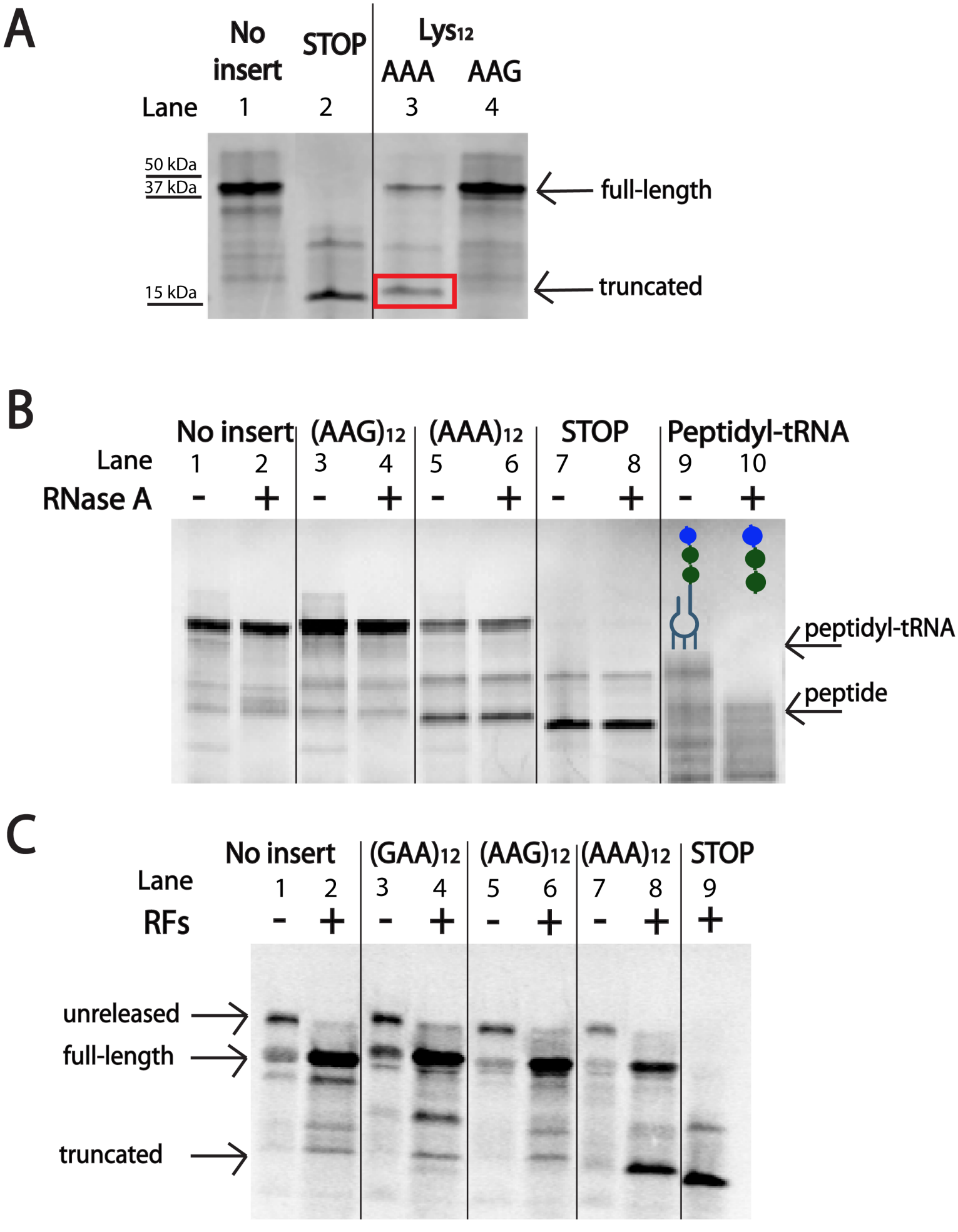
A
No insert
STOP
Lys12
AAA
AAG
Lane
1
2
3
4
50 kDa
37 kDa
15 kDa
full-length
truncated
B
No insert
(AAG)12
(AAA)12
STOP
Peptidyl-tRNA
Lane
1
2
3
4
5
6
7
8
9
10
RNase A
-
+
-
+
-
+
-
+
-
+
peptidyl-tRNA
peptide
C
No insert
(GAA)12
(AAG)12
(AAA)12
STOP
Lane
1
2
3
4
5
6
7
8
9
RFs
-
+
-
+
-
+
-
+
+
unreleased
full-length
truncated

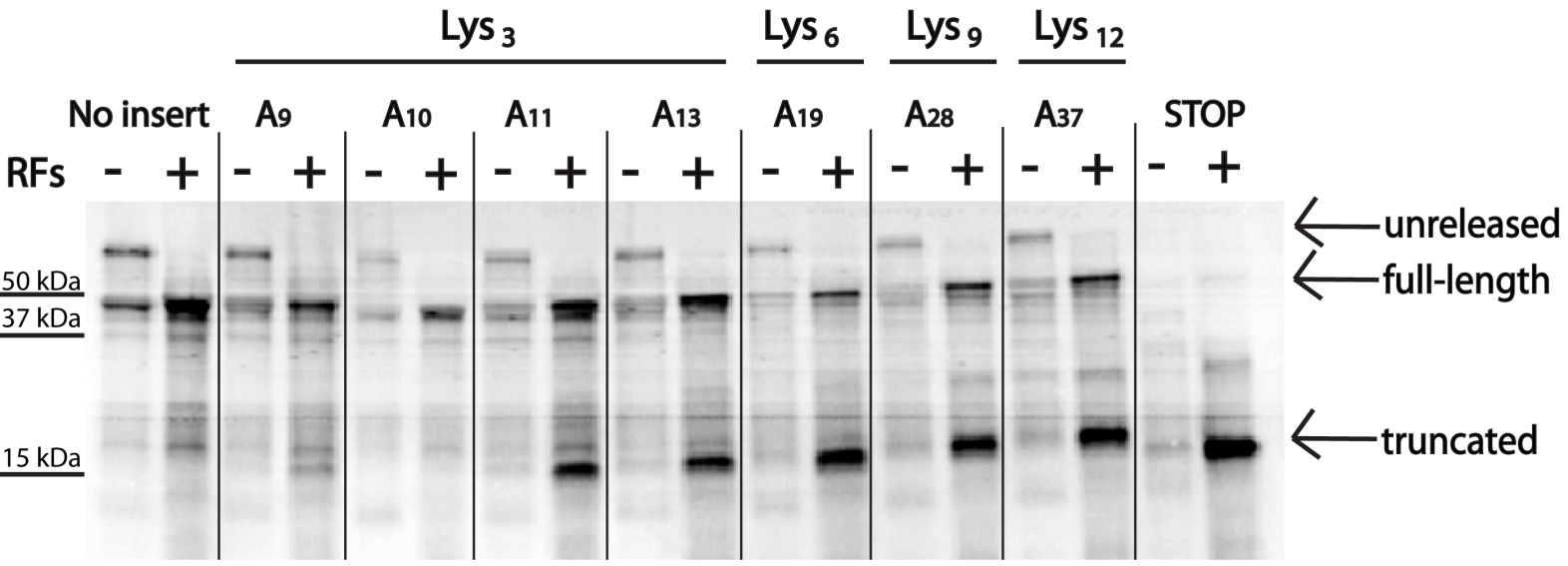
Lys 3
Lys 6
Lys 9
Lys 12
No insert
A9
A10
A11
A13
A19
A28
A37
STOP
RFs
- + - + - + - + - + - + - + - + - +
50 kDa
37 kDa
15 kDa
unreleased
full-length
truncated

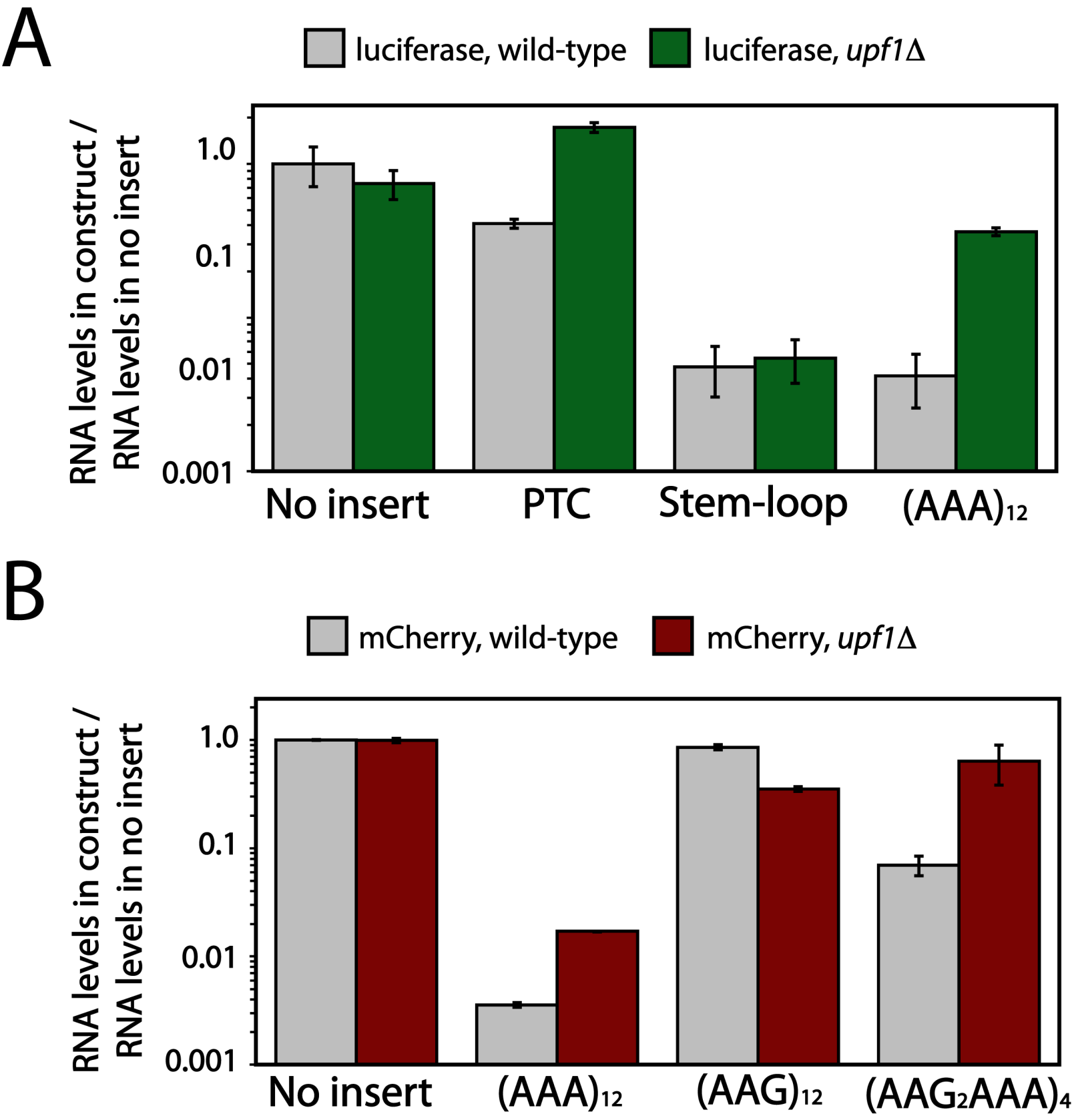
A
luciferase, wild-type
luciferase, upf1Δ
RNA levels in construct / RNA levels in no insert
1.0
0.1
0.01
0.001
No insert
PTC
Stem-loop
(AAA)12
B
mCherry, wild-type
mCherry, upf1Δ
RNA levels in construct / RNA levels in no insert
1.0
0.1
0.01
0.001
No insert
(AAA)12
(AAG)12
(AAG2AAA)4

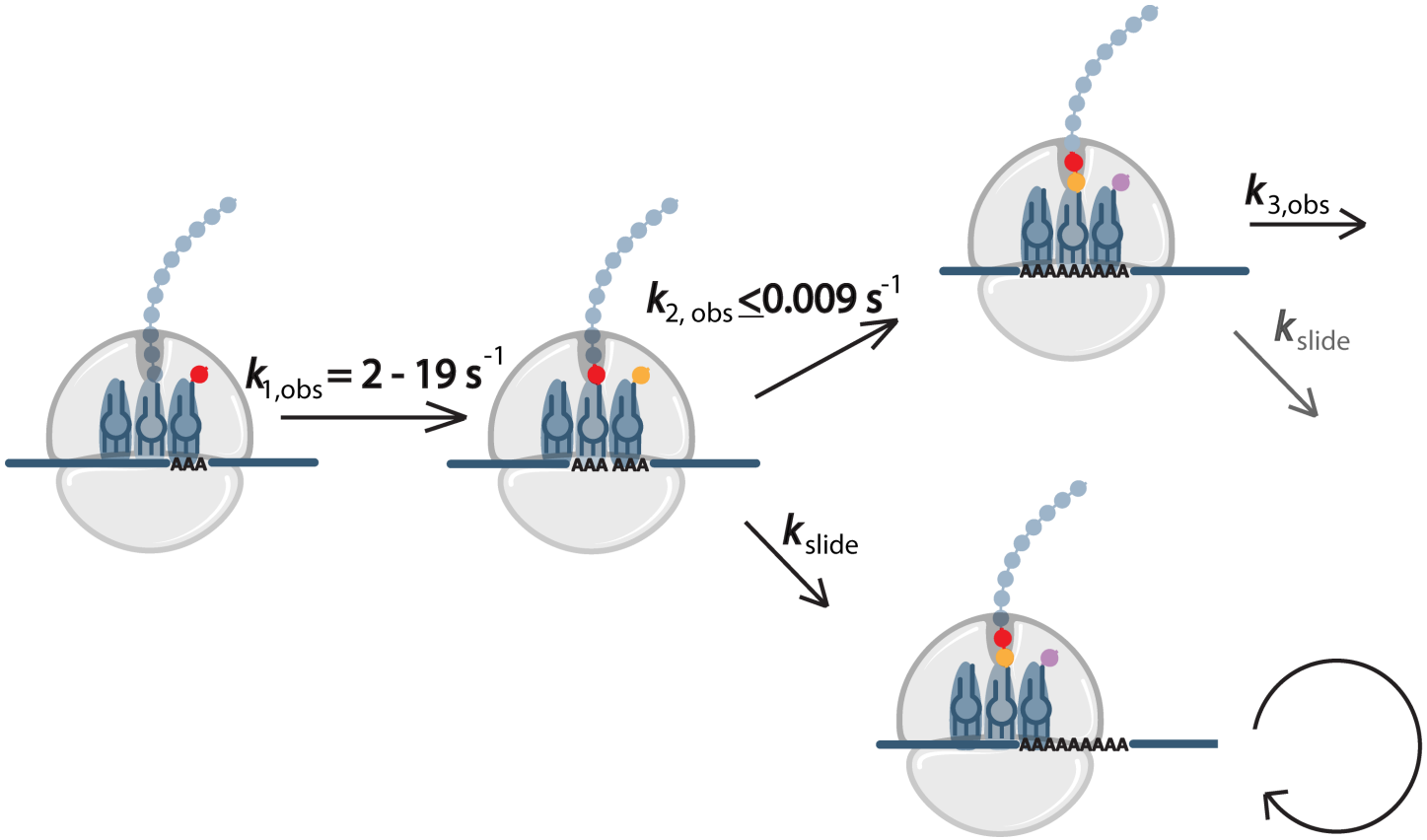
AAA
AAA AAA
AAAAAAAAA
AAAAAAAAA
$k_{1,obs} = 2 - 19\ s^{-1}$
$k_{2,\ obs} \leq 0.009\ s^{-1}$
$k_{3,obs}$
$k_{slide}$
$k_{slide}$